



Field investigation of a multi-helix pile under tensile axial cyclic loading

A. R. F. Christoni

University of São Paulo, São Carlos, Brazil

J. M. S. M. Santos Filho, T. S. O. Morais, C. H. C. Tsuha*

University of São Paulo, São Carlos, Brazil

*chctsuha@sc.usp.br (corresponding author)

ABSTRACT: Helical piles have been proposed as a foundation solution for offshore wind turbines, particularly for jacket structures and anchoring, due to their numerous advantages, including high uplift capacity, minimal environmental impact during installation, and reusability, among others. Offshore foundations and anchors are subjected to cyclic loading from wind, waves, and currents. Most existing studies on helical piles for offshore applications focus on the monotonic performance of single-helix piles, while the cyclic performance of multi-helix piles remains largely unexplored. To address this gap, the current study focuses on the tensile cyclic and post-cyclic behaviour of a four-helix pile. For this purpose, cyclic and monotonic loading tests were conducted on a four-helix pile in a sandy silt soil. To evaluate the load-transfer mechanism during the tests, strain gauges were installed on the pile, enabling the separation of the contributions of the shaft and helical plates to the overall pile performance. For this study, 50 tensile axial loading cycles were applied to the test pile with Q_{min} of $\sim 13\%$ Q_T , and Q_{max} of 50% Q_T , where Q_T is the pile uplift capacity. The main findings from the tests are: (i) a top-down loading transfer mechanism was observed for the monotonic and cyclic tests; (ii) greater displacement accumulation occurred during the first cycles; (iii) the 50 tensile cycles have improved the pile monotonic response.

Keywords: Helical pile; field tests; tensile axial cyclic loading; uplift capacity; load transfer

1 INTRODUCTION

The use of helical piles as foundations or anchors for offshore structures has gained significant attention due to their versatility and efficiency due to the anchor effect of the helix. These piles are easy to install and can be applied in a variety of soil conditions, even in hard-to-reach locations. They have a minimal environmental impact during installation and can be reused. Additionally, helical piles can be loaded immediately after installation, with the installation torque measured used to verify the pile's capacity (Perko, 2009).

In offshore environments, cyclic loads from waves and winds can significantly affect the lifespan of foundations and anchors, potentially leading to a loss of capacity and even fatigue failure due to accumulated displacements over multiple cycles. However, the effects of cyclic loading are often neglected in routine design, despite their significant influence on the foundation's behaviour (Tsuha et al., 2012). In the case of helical piles, the post-cyclic uplift response can be stiffer, as the soil above the helical plates is disturbed during installation, and the

loading cycles may improve this condition. Therefore, studying the cyclic performance of these foundations is crucial for understanding their behaviour and recommending them for offshore foundation applications. Helical foundations have also been successfully used onshore to anchor guy lines of transmission towers, which experience cyclic tensile axial loads throughout their service life due to wind-induced forces on the structures.

Many studies have investigated the cyclic performance of single-helix piles using geotechnical centrifuges, including research by Schiavon et al. (2018), Wang et al. (2024), and Wang et al. (2025). However, field studies on this topic remain limited, with existing research primarily focused on the cyclic behaviour of single-helix piles (Schiavon et al., 2019) and two-helix piles (Costa & Costa, 2019).

For the current study, tensile axial cyclic loading and post-cyclic static monotonic load tests were conducted on a four-helix pile (HP04) installed in a sandy silt soil site. The post-cyclic behaviour was compared to a monotonic tensile test performed in another identical reference virgin pile (RP04), which

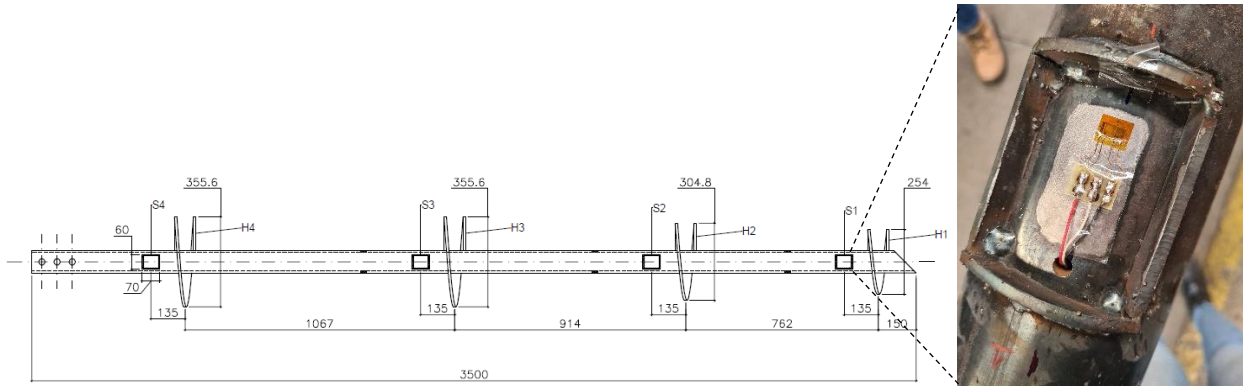


Figure 1. Details of the lead section of the tested helical pile (dimensions in mm) and of an instrumented section.

was installed at the same site, at a horizontal distance of 1.5 meters (axis-to-axis) from pile HP04. Four sections of these piles were instrumented with strain gauges to separate the shaft and helices responses during the loading tests. The main objectives of this study were to evaluate the load-transfer mechanism during cyclic and post-cyclic monotonic loading tests of multi-helix piles, and to assess its the pile head accumulated displacement after a number of cycles with a certain load amplitude, in order to contribute to the design of helical piles as an alternative for offshore wind foundation.

2 HELICAL PILES CHARACTERISTICS

For this study, two helical piles (HP04 and RP04) with four tapered helices (H1 to H4) was used, welded to the lead section with a length of 3.5 meters. The lead section were made of a steel pipe with a diameter of 101.6 mm and a wall thickness of 7.1 mm, while the four helical plates had a thickness of 12.7 mm. The space between the helical plates is three times the diameter (D) of the lower helix. This 3D spacing represents the transition from the cylindrical shear to the individual bearing failure mechanism. The diameters of the helices are as follows: 254.0 mm for H1, 302.8 mm for H2, and 355.6 mm for H3 and H4, as shown in Figure 1.

Four sections (S1 to S4, also indicated in Figure 1), located 135 mm above the helices, were instrumented with bi-axial strain gages in a Wheatstone full bridge configuration. They were positioned in pairs diametrically opposite to each other along the shaft longitudinal axis. The circuit of each section was connected by cables inside the shaft to a HBM (Hottinger Baldwin Messtechnik GmbH) PMX data acquisition system.

Before pile installation the instrumented sections with strain gages were calibrated in

laboratory using a hydraulic jack. Strain measurements were correlated with applied load, and the equations were used in the acquisition system, enabling the determination of the tensile load acting axially on the shaft just above each helix during the cyclic and monotonic loading tests.

The installation of the piles was carried out using a hydraulic motor. The applied torque was measured every 0.5 meters of pile penetration into the ground using a digital torque meter. The two piles tested in this work have embedded length of 13.3 meters, with final installation torque of 15.9 kN.m for HP04, and 15.6 kN.m for RP04.

3 SOIL CHARACTERIZATION

The piles were installed at a site located in the city of Contagem, Brazil, at coordinates 19° 55' 54" S latitude and 44° 03' 13" W longitude. Soil samples taken from an SPT borehole near the pile indicate that the soil consists of a silty clay layer from 0 to 3 meters deep, followed by another silty clay layer extending to 6 meters, and a sandy silt layer reaching down to 30.5 meters. The groundwater level was found at a depth of 13.3 meters below the ground surface. Figure 2a shows the soil profile at the test site. Figure 2b presents the results of a Standard Penetration Test (SPT) with 72% hammer efficiency. Figure 2c shows the results of a Cone Penetration Test (CPT), and Figure 2d illustrates the results of pile installation torque.

4 CYCLIC PERFORMANCE

Fifty tensile loading cycles were conducted on helical pile HP04, followed by a monotonic tensile load test (post-cyclic). The cyclic parameters were: Q_{min} of $\sim 13\% Q_T$, and Q_{max} of $0.5 Q_T$, where Q_T is the tensile pile capacity from a monotonic loading test performed on reference pile (RP04).

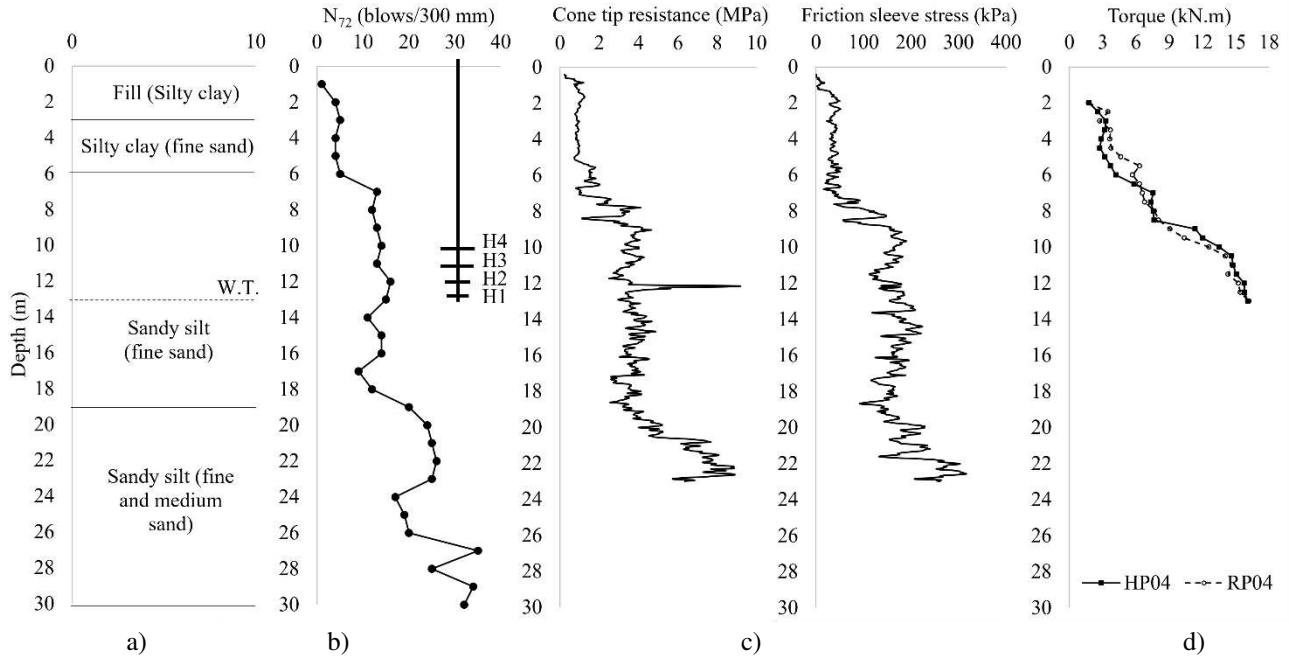


Figure 2. a) Soil Profile of experimental site at Contagem; b) results of SPT; c) results of CPT; d) results of installation torque of piles RP04 and HP04.

The loads were applied using a hydraulic jack with a 931 kN capacity (Enerpac Corp., type RRH1006, 153 mm stroke, Double-acting, Hollow Plunger Hydraulic Cylinder), connected to an electric pump. Load measurements were recorded using an HBM C6B load cell with a nominal force of 2 MN. Displacement readings were obtained with four Linear Variable Differential Transformer (LVDT) devices with a 100 mm stroke (HBM type WA-T/100), as shown in Figure 3.

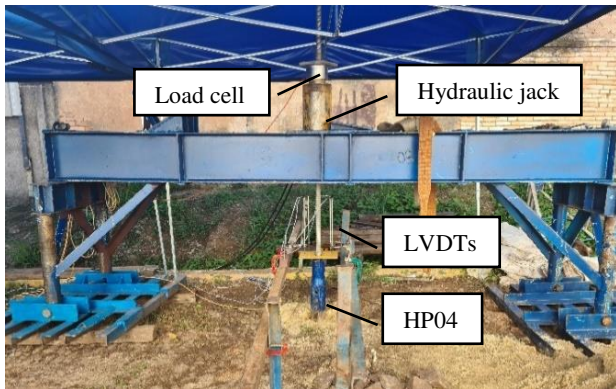


Figure 3. Pile load tests set-up.

Table 1 shows the condition adopted for the cyclic tests on pile HP04, considering $Q_{mean} = (Q_{max} + Q_{min})/2$ and $Q_{cyclic} = (Q_{max} - Q_{min})/2$. Figure 4 illustrates the applied tensile load during the cyclic test.

Based on the pile instrumentation results and the calibration equations, the loads acting on sections S1 to S4, just above the helices, were determined as

presented in Table 2, and in the load transfer diagram of Figure 5, indicating the maximum and minimum tensile load applied to the pile head, during the first and the last load cycle (cycles 1 and 50).

Table 1. Characteristics of the tensile cyclic load test on the pile HP04.

Load (Q)	(kN)	Q/Q_T
Q_{min}	50	~0.13
Q_{max}	190	0.50
Q_{mean}	120	~0.32
Q_{cyclic}	70	~0.18
Q_T	380	1.00

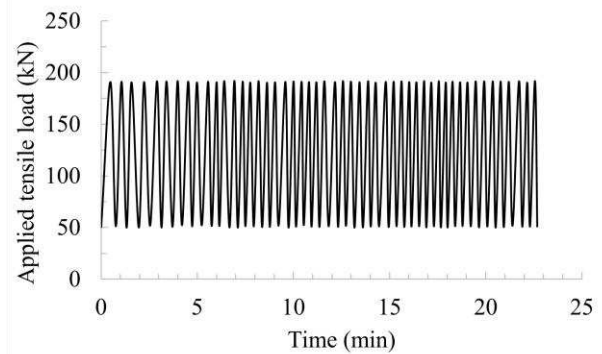


Figure 4. Applied tensile load vs time during the cyclic test on pile HP04.

The shaft resistance mobilized during the test corresponds to the applied load at the pile head minus the load recorded at the section S4 (Figure 1).

Table 2. Tensile load values measured at the pile head and just above the helices during the cyclic loading.

Instrument. position	Depth (m)	Cycle 1 min (kN)	Cycle 50 min (kN)	Cycle 1 max (kN)	Cycle 50 max (kN)
Pile head	0.00	50.6	50.9	190.8	191.7
above H4	10.26	36.5	60.0	151.8	153.0
above H3	11.33	28.0	36.6	90.6	87.0
above H2	12.24	15.6	23.9	72.9	66.5
above H1	13.01	0.0	4.6	31.7	24.7

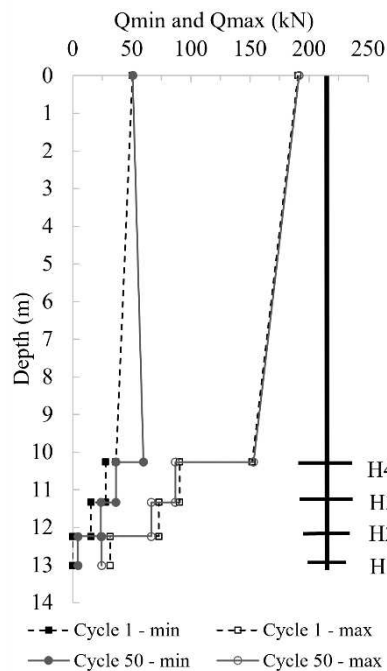


Figure 5. Load transfer during cycles 1 and 50.

A top-down loading transfer mechanism was observed during the cyclic tests. At the maximum tensile load (190 kN), the load distribution along the helical pile show that a higher portion of the tensile load is resisted by the helical plates (~20% of the maximum load applied is resisted by the shaft). Additionally, for the level of load applied ($Q_{max} = 50\%$ of pile tensile capacity) no degradation in shaft resistance is observed for Q_{max} between the first and last cycles.

The top helix showed the greatest contribution compared to the other helices. The results of Figure 5 suggest that the helix 3 was likely installed in a soil layer with lower resistance compared to the helix 2. In Figure 2, the N_{72} and q_c values show a slight reduction at a depth of -11m (the depth of helix 3) compared to the depth of the helix 2. The vertical variability in the residual soil resistance also contributes to the variation in the load carried by each helix. Additionally, during the last cycle (cycle 50) at the minimum load, the load registered above the top helix is 10 kN higher than the load applied to

the pile head (50 kN), indicating both negative skin friction and residual stresses above the top helix.

With the measured loads at each instrumented pile section (S1 to S4) above the helices, it was possible to determine the load mobilized by each helix during the loading cycles. The load resisted by H4 (top helix) corresponds to the load registered at S4 minus the load registered at S3. The load resisted by H3 corresponds to the load registered at S3 minus the load registered at S2. The load resisted by H2 corresponds to the load registered at S2 minus the load registered at S1. The load resisted by H1 is the load registered at S1. The shaft resistance between the helices was not considered (shadow effects). Figure 6a-d presents the variation of load mobilized by the helices 1 (bottom), 2, 3, and 4 (top helix), during the cyclic load performed on HP04.

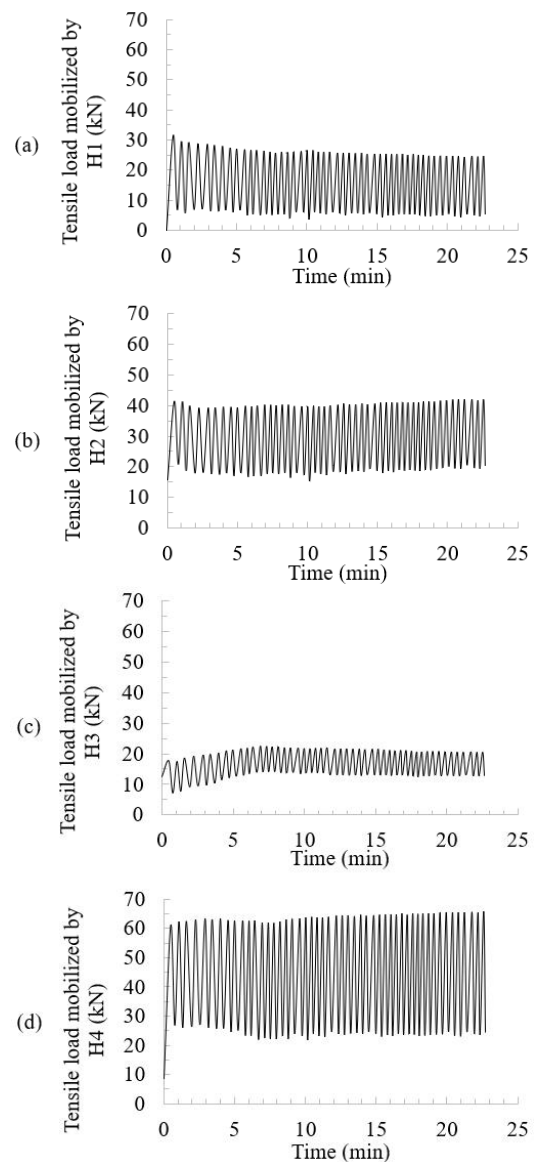


Figure 6. Tensile load resisted by the helices 1(a), 2(b), 3(c) and 4(d) during the cyclic test on the pile HP04.

The duration of the cyclic load test was approximately 23 minutes. As illustrated in Figure 6, the lowest load amplitude was observed at the instrumented section just above helix H3 (ranging from 10 to 20 kN), while the largest load amplitude was recorded just above the top helix H4 (ranging from 20 to 70 kN). The load amplitude above the bottom helix H1 varied from 5 to 30 kN, and above helix H2, it ranged from 20 to 40 kN.

Figure 7 illustrates that the largest displacement occurs during the first cycle. In the initial stages of cyclic loading (the first 10 cycles), there is a significant accumulation of displacement, likely due to the compaction of soil previously disturbed by the passage of the helices during pile installation. Following this, the rate of displacement increase slows down. This indicates that the applied cyclic loading was able to improve the soil above the helix, compacting it and reducing the accumulated displacements (Spagnoli and Tsuha, 2020).

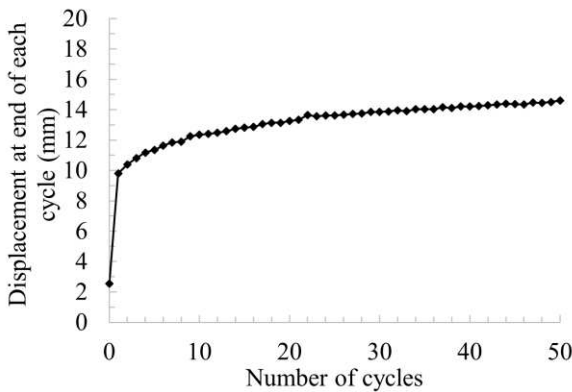


Figure 7. Permanent displacement results at the end of each cycle (Q_{min}) during the cyclic test on pile HP04.

5 POST-CYCLIC CAPACITY

After cyclic loading, a monotonic tensile load test was conducted on the helical pile HP04, using the quick load test procedure as described in ASTM D3689 (ASTM, 2007). A monotonic tensile load test was also conducted on the reference pile (RP04) for comparison.

Thirteen equal load increments of 27 kN (corresponding to 10% of a calculated pile uplift capacity of 270 kN before testing) were applied to the pile head during the tests. Two loading cycles were conducted for each test, and the resulting load-displacement curves are shown in Figure 8. As no clear failure was observed during the two monotonic load tests, the pile uplift capacity values were calculated by extrapolating the best fit curve of the test data, and using the criteria presented in Livneh and El Naggar (2008) (load equivalent to the

pile head displacement equal to 8% of the largest helix diameter plus the elastic deflection of the pile).

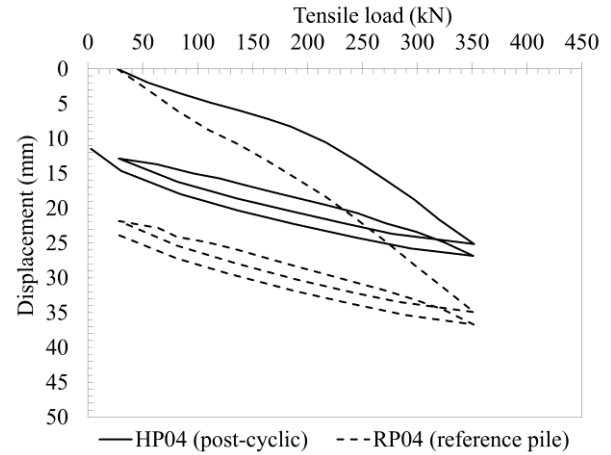


Figure 8. Tensile load-displacement curves of monotonic loading tests on pile RP04 and after cycles on pile HP04.

The pile uplift capacity (Q_T) obtained for RP04 was 380 kN, while the post-cyclic capacity, obtained for HP04, was 430 kN. Although the exact failure load values are uncertain, as they are derived through extrapolation, the enhancement in the pile's response after 50 cycles of cyclic loading is primarily evident in the improved load-displacement behavior and increased stiffness.

A comparison in Figure 9 was made between the load transfer of a 'virgin' reference pile (which had not undergone any load cycles) and a pile that had previously experienced cyclic loading.

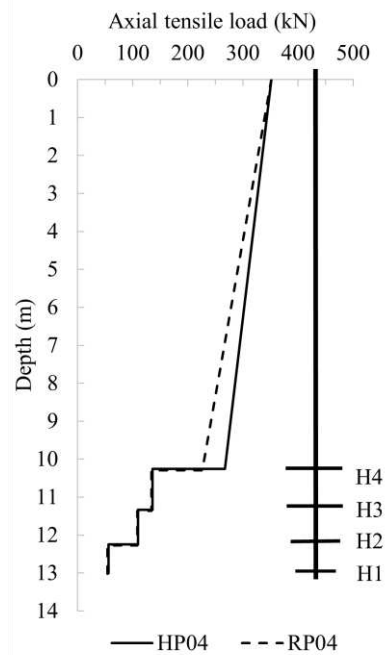


Figure 9. Load transfer at the end of the monotonic tests on pile RP04 and on pile HP04 after cyclic loading.

The two piles of Figure 9 are identical, with the same embedded length and similar final torque (indicating same soil condition). Additionally, the uplift bearing capacities of helices 1, 2, and 3 are identical, as shown in Figure 9. The objective of the two monotonic loading tests was to assess whether the 50 load cycles caused any degradation in the pile's shaft resistance and whether the soil above Helix 4 was improved after cyclic loading. This figure indicates a combination of shaft degradation and an improvement in the uplift bearing capacity of Helix 4. According to Victor and Cerato (2008), repeated load applications tend to enhance the post-cyclic capacity of a helical pile by stiffening the soil-anchor system.

6 CONCLUSIONS

A tensile cyclic loading test followed by a post-cyclic monotonic loading was conducted on an instrumented four-helix pile.

Although the pile response presented in this paper is related to a multi-helix pile tested in a specific unsaturated soil site, with a lower number of cycles compared to offshore applications, and a unique combination of cyclic parameters (Q_{\max} equivalent to $0.5 Q_T$, load with a safety factor of 2.0), the results indicate a top-down loading transfer mechanism during both cyclic and monotonic tests, with a significant contribution from the helical plates compared to the shaft resistance.

Additionally, larger displacements occur during the initial cycles, with a reduction in accumulated displacements in the later cycles. For the tested cyclic conditions and number of cycles, the applied cyclic loading enhanced the soil above the top helix and improved the monotonic pile tensile load-displacement response and stiffness, compared to the virgin pile.

AUTHOR CONTRIBUTION STATEMENT

First Author: Conceptualization, Data curation, Formal Analysis, Writing- Original draft. **Second and Third Authors:** Methodology, Visualization, **Last Author:** Supervision, Project administration, Validation, Writing- Reviewing and Editing,

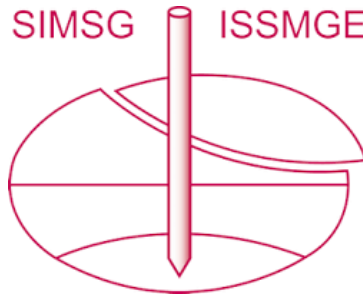
ACKNOWLEDGEMENTS

The authors are grateful for the financial support provided by Neoenergia Group and the ANEEL P&D Program (Project PD-07284-0002/2020).

REFERENCES

- ASTM D3689 (2007). Standard test method for individual piles under static axial tensile load. West Conshohocken, PA, USA: ASTM International.
- Costa, J. P., & Costa, Y. D. (2019). Cyclic Stability of Helical Anchors Installed in a Sedimentary Sand Deposit. In *Geotechnical Engineering in the XXI Century: Lessons learned and future challenges* (pp. 928-935). IOS Press.
- Livneh, B.; El Naggar, M. H. (2008). Axial testing and numerical modeling of square shaft helical piles under compressive and tensile loading. *Canadian Geotechnical Journal*, 45(8), pp. 1142-1155.
- Perko, H. A. (2009). Helical Piles. Hoboken, New Jersey: John Wiley & Sons.
- Schiavon, J. A.; Tsuha, C. H. C.; Neel, A.; Thorel, L. (2018). Centrifuge modelling of a helical anchor under different cyclic loading conditions in sand. *International Journal of Physical Modelling in Geotechnics*.
- Schiavon, J. A.; Tsuha, C. H. C.; Thorel, L. (2019). Monotonic, cyclic and post-cyclic performances of single-helix anchor in residual soil of sandstone. *Journal of Rock Mechanics and Geotechnical Engineering*, 11 (4), pp. 824-836.
- Spagnoli, G.; Tsuha, C. H. C. (2020). A review on the behavior of helical piles as a potential offshore foundation system. *Marine Georesources & Geotechnology*.
- Tsuha, C. H. C.; Foray, P. Y.; Jardine, R. J.; Yang, Z. X.; Silva, M.; Rimoy, S. (2012). Behaviour of displacement piles in sand under cyclic axial loading. *Soils and Foundations*, 52 (3), pp. 393-410.
- Victor, R. T.; Cerato, A. B. (2008). Helical anchors as wind tower guyed cable foundations. *Proceedings of the Second BGA International Conference on Foundations, ICOF2008*.
- Wang, W.; Brown, M. J.; Sharif, Y. U.; Davidson, C.; Ciantia, M. O. (2024). Centrifuge modelling of two-way axial cyclic response of screw piles for offshore wind. *Proceedings of the 5th European Conference on Physical Modelling in Geotechnics*.
- Wang, W., Brown, M. J., Sharif, Y. U., Davidson, C., & Ciantia, M. O. (2025). Centrifuge Modeling of the Installation Advancement Ratio Effect on the Cyclic Response of a Single-Helix Screw Pile for Floating Offshore Wind. *Journal of Geotechnical and Geoenvironmental Engineering*, 151(1), 04024133.

INTERNATIONAL SOCIETY FOR SOIL MECHANICS AND GEOTECHNICAL ENGINEERING



This paper was downloaded from the Online Library of the International Society for Soil Mechanics and Geotechnical Engineering (ISSMGE). The library is available here:

<https://www.issmge.org/publications/online-library>

This is an open-access database that archives thousands of papers published under the Auspices of the ISSMGE and maintained by the Innovation and Development Committee of ISSMGE.

The paper was published in the proceedings of the 5th International Symposium on Frontiers in Offshore Geotechnics (ISFOG2025) and was edited by Christelle Abadie, Zheng Li, Matthieu Blanc and Luc Thorel. The conference was held from June 9th to June 13th 2025 in Nantes, France.